

Characterization of thin ZrO₂ films deposited using (ZrO₂ - Pr)₂(thd)₂ and O₂ on Si(100)

H.-W. Chen, D. Landheer, X. Wu, S. Moisa, G. I. Sproule, T.-S. Chao, and T.-Y. Huang

Citation: *Journal of Vacuum Science & Technology A* **20**, 1145 (2002); doi: 10.1116/1.1467358

View online: <http://dx.doi.org/10.1116/1.1467358>

View Table of Contents: <http://scitation.aip.org/content/avs/journal/jvsta/20/3?ver=pdfcov>

Published by the AVS: Science & Technology of Materials, Interfaces, and Processing

Articles you may be interested in

[Ionic conductivity of co-doped Sc₂O₃ - ZrO₂ ceramics](#)

AIP Conf. Proc. **1461**, 289 (2012); 10.1063/1.4736906

[Luminescence and visible upconversion in nanocrystalline ZrO₂ : Er³⁺](#)

Appl. Phys. Lett. **83**, 4903 (2003); 10.1063/1.1632020

[Luminescent properties and energy transfer in ZrO₂ : Sm³⁺ nanocrystals](#)

J. Appl. Phys. **94**, 3509 (2003); 10.1063/1.1599960

[Effect of crystal nature on upconversion luminescence in Er³⁺ : ZrO₂ nanocrystals](#)

Appl. Phys. Lett. **83**, 284 (2003); 10.1063/1.1592891

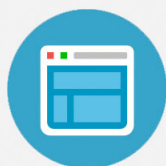
[Miscibility of amorphous ZrO₂ - Al₂O₃ binary alloy](#)

Appl. Phys. Lett. **80**, 2374 (2002); 10.1063/1.1459765



Re-register for Table of Content Alerts

Create a profile.



Sign up today!



Characterization of thin ZrO₂ films deposited using Zr(Oⁱ-Pr)₂(thd)₂ and O₂ on Si(100)

H.-W. Chen^{a)}

Institute of Electronics Engineering, National Chiao-Tung University, Hsinchu 300, Taiwan, Republic of China

D. Landheer, X. Wu, S. Moisa, and G. I. Sproule

Institute for Microstructural Sciences, National Research Council of Canada, Ottawa, Ontario K1A 0R6, Canada

T.-S. Chao^{b)}

Department of Electrophysics, National Chiao-Tung University, Hsinchu 300, Taiwan, Republic of China

T.-Y. Huang^{b)}

National Chiao-Tung University, Hsinchu 300, Taiwan, Republic of China

(Received 9 August 2001; accepted 11 February 2002)

The properties of ZrO₂ films deposited using molecular oxygen and a recently developed precursor, zirconium Zr(Oⁱ-Pr)₂(thd)₂ have been investigated. The organometallic was dissolved as a 0.15 molar solution in octane and introduced into the deposition chamber using a liquid injection system. The deposition rate was insensitive to molecular oxygen flow but changed with liquid injection rate and was thermally activated in the range 390 °C–550 °C. Carbon concentrations, <0.1 at. %, the detection limit of the x-ray photoelectron spectroscopy depth profiling measurements, were obtained at the lowest deposition temperatures and deposition rates. High-resolution transmission electron microscopy showed the films to be polycrystalline as deposited, with a zirconium silicate interfacial layer. After proper annealing treatments, an equivalent oxide thickness (EOT) of around 2.3 nm has been achieved for a 5.2 nm thick film, with a leakage current two orders of magnitude lower than that of SiO₂ with the same EOT. Promising capacitance–voltage characteristics were also achieved, but some improvements are required if these films are to be used as a gate insulator. © 2002 American Vacuum Society. [DOI: 10.1116/1.1467358]

I. INTRODUCTION

As the dimensions of complementary metal oxide semiconductor (CMOS) devices are scaled in the deep submicron regime, the thickness of the required gate dielectric will steadily decrease to dimensions <1 nm.¹ For SiO₂, however, the large resulting direct tunneling currents result in large power consumption and reduced reliability.^{2,3} With higher dielectric constant, κ , the gate insulator thickness can increase, while maintaining the equivalent oxide thickness (EOT), and reducing significantly the tunneling leakage current. Thus, in recent years, high- κ materials which are predicted to be thermodynamically stable with Si,⁴ such as ZrO₂, HfO₂, La₂O₃, Al₂O₃, and their silicates have been considered as candidates for alternative gate dielectrics.⁵ ZrO₂ is a candidate because of its high dielectric constant (~25), high bandgap energy (5.8–7.8 eV),^{5,6} and thermal compatibility with contemporary CMOS processes.^{7–9}

Although electron-beam evaporation or sputtering are useful techniques for depositing new materials for evaluation, they can damage electrical devices, have difficulties with uniformity and purity and are hard to maintain in production. Thus chemical vapor deposition (CVD) is usually preferred and, in this article, metalorganic CVD (MOCVD) was used to deposit ZrO₂. A mature MOCVD process re-

quires precursors, stable upon exposure to atmosphere, to replace the moisture- and air-sensitive chloride or alkoxide precursors usually employed. This article reports the investigation of the physical and electrical properties of thin ZrO₂ films deposited using molecular oxygen and a recently developed precursor, zirconium Zr(Oⁱ-Pr)₂(thd)₂ (Oⁱ-Pr is isopropoxide and thd is 2,2,6,6-tetramethyl-3,5-heptanedionate)¹⁰ introduced into the chamber with a liquid injection system. Pure, stoichiometric ZrO₂ films have been deposited and the effects of postdeposition annealing have been investigated. Low leakage current density–voltage (J - V) characteristics and capacitance–voltage (C - V) characteristics with small hysteresis have been demonstrated.

II. EXPERIMENT

Si(100) substrates, 100 mm diameter, n -type (ρ = 0.02–0.06 Ω cm) were given a HF-last Radio Corporation of America clean prior to film deposition. The CVD chamber is equipped with a 360 l/s turbomolecular pump and a liquid injection system. The latter consisted of a liquid pump to pump the precursor, a 0.15 molar solution of Zr(Oⁱ-Pr)₂(thd)₂ in octane, through a hot nickel frit at a rate of 0.2 ml/min. The vapors were carried with a 50 sccm flow of Ar to a gas distribution ring 10 cm from the substrate. The nickel frit, the components of the vaporizer, the gas ring, and the connecting tube were maintained at a temperature of

^{a)}Electronic mail: hwchen.ee86q@nctu.edu.tw

^{b)}Also at: National Nano Device Laboratories, Hsinchu, Taiwan.

190 °C, while the substrate temperature was controlled in the range 390 °C–550 °C with quartz-halogen lamps and a thermocouple. Oxygen was introduced in the chamber at flow rates of 0–150 sccm through a separate gas distribution ring 30 cm from the substrate. Just prior to deposition the wafers were heated for 10 min at 500 °C in 10 mTorr of O₂ to replace the surface hydrogen termination with oxygen.

Films were analyzed by x-ray photoelectron spectroscopy (XPS) using a PHI 5500 system with a monochromatic Al K α x-ray source in a standard 90° geometry and a band-pass energy of 58.7 eV. Thick films were typically stoichiometric ZrO₂ when analyzed by Rutherford backscattering. Depth profiles of the C 1s peaks showed that the films were contaminated with 1–2 at. % carbon, with the smallest contamination at the lowest temperatures where the deposition rates were lowest.

Since the liquid pump was not sufficiently stable at flow rates below 0.2 ml/min, to reduce deposition rates and further reduce the carbon contamination, subsequent depositions were done in “pulse mode” in which the precursor and oxygen were introduced separately with intervening pumping periods of 15 s. Nitrogen at a flow rate of 100 sccm was introduced into the oxygen gas ring and flowed during the complete deposition cycle. Thus each cycle of deposition consisted of four stages: 100 sccm N₂, 150 sccm O₂+100 sccm N₂, 100 sccm N₂, and 50 sccm Ar+100 sccm N₂+Zr precursor (0.2 ml/min). Pressures at various stages of the deposition cycle were in the 8–12 mTorr range.

The depositions were monitored with an *in situ* ellipsometer operating at a wavelength of 633 nm. The ellipsometric angles were used to calculate the deposited film thickness in real time from the known optical constants for Si and assuming the film was uniform, nonabsorbing, and had a refractive index of 2. This results in an approximate thickness measurement that must be calibrated by *ex situ* analysis.

Atomic force microscopy (AFM) measurements were made on the as-deposited and annealed samples using a Digital Instruments Nanoscope III operating in tapping mode with 5 nm diameter silicon probes. The structure of the films and the effect of annealing was observed directly in high-resolution transmission electron microscope (HRTEM) micrographs made on a Philips EM-430T instrument operating at 250 keV.

Samples were annealed in a Heatpulse 610 (Steag RTP Systems) rapid thermal processor. For spike anneal in O₂, the temperature was ramped at 125 °C C/s to 800 °C to 900 °C, or 950 °C and held for 1 s. Forming gas anneals (FGAs) were done in a 4% H₂ in N₂ mixture for 10–30 min in the temperature range from 380 °C–600 °C.

For the electrical measurements, Al-gated capacitors were made by evaporating aluminum through a shadow mask and back contacts were made with In–Ga eutectic. The FGAs were done before metal deposition to avoid reaction of the Al with the films. Electrical measurements were made by probing the Al gates in a probe station attached to two instruments, a multifrequency LCR meter (HP Model 4275A) for C–V characteristics, and picoammeter dc voltage source (HP

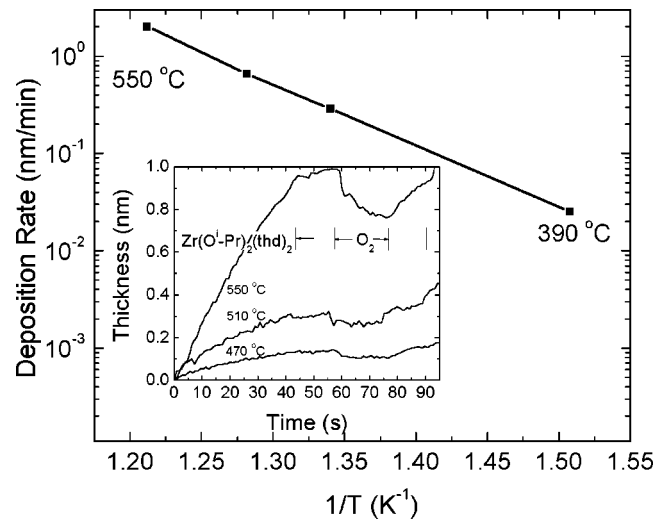


Fig. 1. Logarithmic plot of the deposition rate vs $1/T$. The activation energy determined from the slope is 1.27 eV. The inset shows that film thickness as a function of time obtained from the *in situ* ellipsometer during one cycle of deposition for temperatures substrate temperature 470, 510, and 550 °C.

Model 4140B) for current–voltage characteristics. The equivalent oxide thickness (EOT) was obtained from the 100 kHz C–V characteristics by using the NCSU C–V fitting routine,¹¹ which includes quantum effects in the channel.

III. RESULTS AND DISCUSSIONS

A. Physical characteristics

For our flow parameters, the film thickness depends on the number of deposition cycles, substrate temperature, O₂ time, and precursor injection time. In the range of temperature and pressure investigated here, the film deposition rate did not saturate as the precursor injection time was increased. Furthermore, when the oxygen was turned off the deposition rate did not decrease significantly. This indicates that we were not operating in the atomic layer deposition mode, possibly because background water vapor from the chamber or the process was sufficient to effect the oxidation. Since the Zr is coordinated to six oxygens in the precursor, it is also possible that an oxidant is not necessary to form ZrO₂ with this precursor. However, without oxygen the carbon in the films was significant. With this pulse mode deposition, O₂ can react with the film and reduce the carbon in the film effectively. A plot of the log of the average deposition rate as a function of inverse temperature is shown in Fig. 1. The activation energy determined from the slope of the fit to the data in the range 390 °C–550 °C is 1.27 eV. The thickness from the *in situ* ellipsometer during one cycle is shown in the inset of Fig. 1 for substrate temperatures of 470 °C, 510 °C, and 550 °C. The film thickness increases during the precursor injection but seems to decrease during oxygen flow. The latter decrease is recovered during the subsequent pump down (period with nitrogen flow only) and may be associated with adsorption and desorption of oxygen on the surface.

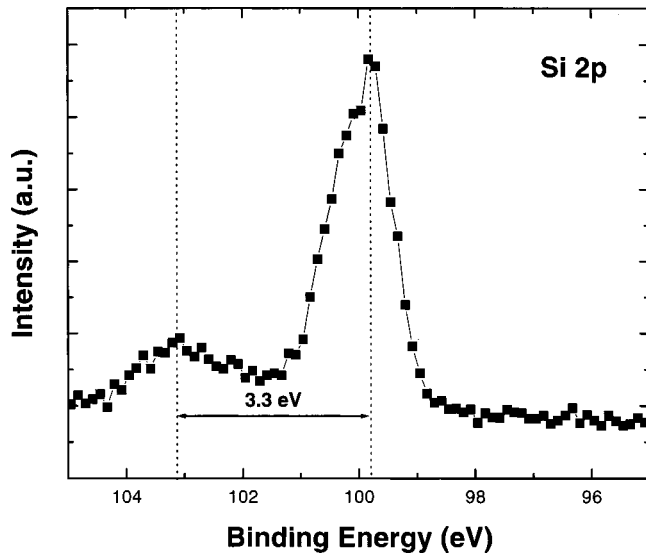


FIG. 2. XPS Si 2*p* spectrum for the as-deposited ZrO₂ film with a TEM thickness of 4.7 nm. The peak near 103 eV shifted 3.3 eV from the substrate peak is associated with a silicate layer at the Si interface.

Figure 2 shows XPS Si 2*p* spectrum of a thin ZrO₂ film deposited with 75 cycles at 390 °C. The peak near the binding energy of ~103 eV is 3.3 eV from the Si substrate peak, a chemical shift smaller than the >4 eV shift observed for 1.8 nm thick SiO₂ films.¹² This is characteristic of a silicate layer consistent with the transmission electron microscopy (TEM) image and *C*–*V* data shown later. A C1*s* peak was visible on the surface of the film, but this disappeared during depth profiling, indicating that the carbon contamination in the bulk of this film is less than the detection limit (estimated to be <0.1 at. %). The root-mean-square surface roughness of this film measured by AFM is 4.4 Å.

Figure 3 shows the HRTEM image of the same film. An amorphous interfacial layer is evident between the substrate and the polycrystalline ZrO₂ layer and this is identified as the silicate layer responsible for the Si 2*p* feature in the XPS spectrum. The interface between silicate and Si is atomically sharp. After spike anneal in O₂ at 850 °C and FGA, the thickness of the silicate layer was increased by 2 Å. This is due to

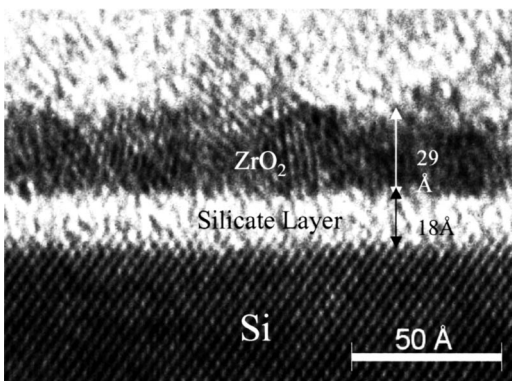


FIG. 3. HRTEM cross section image of film as-deposited on Si(100) at 390 °C.

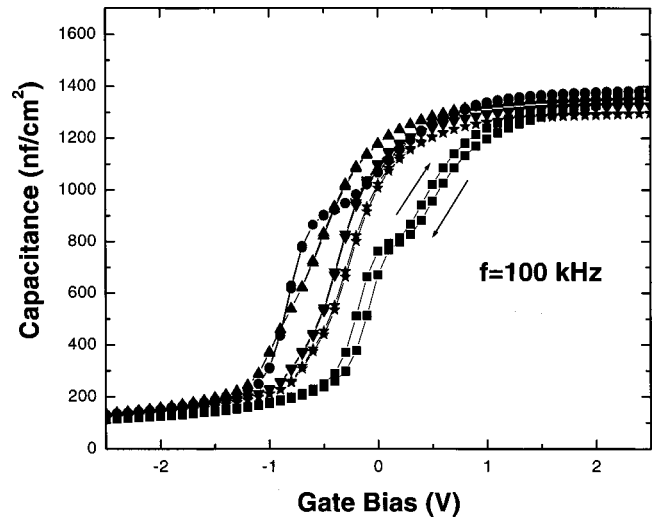


FIG. 4. High frequency *C*–*V* characteristics of capacitors with ZrO₂ gate dielectrics obtained at 100 kHz. The samples were spike annealed for 1 s in O₂ at 850 °C first, then FGA at 380 °C for 10–30 min: (■) no anneals, (●) spike anneal only, (▲) 10 min FGA, (▼) 20 min FGA, and (★) 30 min FGA.

oxygen penetration to the Si substrate since ZrO₂ is a fast ion conductor with significant oxygen ion diffusivity.⁶

Although the silicate layer reduces the effective dielectric constant of the whole gate dielectric, it could reduce the interface state density. It could also improve the carrier mobility in the channel of a metal–oxide–semiconductor field-effect transistor⁸ by providing a smoother interface in direct contact with the Si substrate.

B. Electrical characteristics

The 100 kHz *C*–*V* characteristics of ZrO₂ films deposited using 75 deposition cycles are shown in Fig. 4 for different annealing treatments. For the as-deposited sample, there is a significant hump in the *C*–*V* curve in accumulation most likely associated with *P_b* centers.¹³ A flatband voltage $V_{FB} = -0.06$ V (scan from inversion to accumulation) corresponding to a large negative fixed charge density ($N_f = -1.1 \times 10^{12}/\text{cm}^2$), and a significant clockwise hysteresis ($\Delta V_{FB} \sim 0.21$ V) associated with charge trapping and detrapping are also observed. For the sample spike annealed for 1 s in O₂ at 850 °C, the flatband voltage shifts from -0.06 to -0.76 V ($N_f = 6.0 \times 10^{12}/\text{cm}^2$), and the hysteresis becomes smaller. Some samples spike annealed at 850 °C for 1 s in O₂ were subsequently given an FGA at 380 °C, which passivated the *P_b* centers. For the 20 min FGA, the charge associated with the hysteresis, ΔN_t , is reduced to $5.0 \times 10^{10}/\text{cm}^2$, where ΔN_t is the effective density of trapped charge. For the 30 min FGA, the flatband voltage shifts toward the ideal flatband voltage (ideal $V_{FB} \sim -0.2$ V).¹⁴ The fixed charge density is reduced to $2.6 \times 10^{11}/\text{cm}^2$ and this may be due to the introduction of negative fixed charge or the annealing of the positive fixed charge. However, the hysteresis is increased by 10%, so there appears to be a trade off between trapped and fixed charge.

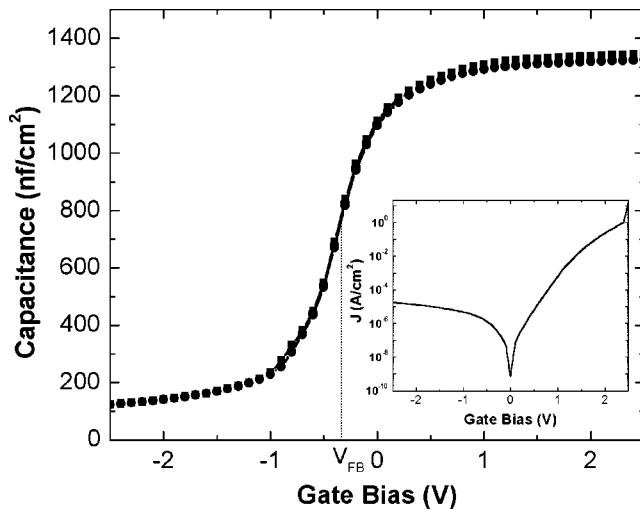


Fig. 5. Frequency dependence of the C - V characteristics of a ZrO₂ film on n^+ Si with an EOT of 2.27 nm after spike anneal at 850 °C in O₂ for 1s and FGA at 380 °C for 20 min: (■) 10 kHz, (●) 100 kHz. A slight frequency dispersion is evident below midgap. The hysteresis ($\Delta V_{FB} \sim 6$ mV) is small. The inset shows the corresponding J - V curve, which is asymmetric and has a leakage current density of 6×10^{-4} A/cm² at 1 V (substrate injection).

Figure 5 shows the 10 kHz and 100 kHz C - V characteristics and the J - V characteristics of the sample spike annealed and annealed in forming gas for 20 min. From the 100 kHz C - V curve, the EOT is 22.7 Å, with the quantum correction, corresponding to $\kappa = 9.3$. This is lower than that of ZrO₂ due to the interfacial silicate layer. In addition, there is slight frequency dispersion in the C - V curves, mainly below midgap. The inset to Fig. 5 shows the asymmetric J - V curve measured with light illumination for the same sample. The leakage current densities are 6×10^{-4} A/cm² at 1 V and 4.7×10^{-6} A/cm² at -1 V. For a pure SiO₂ film with an EOT 22.7 Å, the leakage current density is about two orders of magnitude larger for a gate potential $V_G = V_{FB} + 1$ V.³ However, the leakage is larger than expected from tunneling, Frenkel-Poole conduction, or Schottky emission.¹⁵ This might be due to the difference of the barrier heights under different voltage polarity or might be due to a peaked distribution of traps in the dielectric that favors trap-assisted tunneling for substrate injection.¹⁶ Further investigation of the leakage mechanism is necessary but reducing the film surface roughness observed by HRTEM and AFM should improve performance.

IV. CONCLUSIONS

In this work it has been shown that thin stoichiometric, carbon-free ZrO₂ films can be deposited on Si(100) using the novel precursor Zr(O^{*i*}-Pr)₂(thd)₂ dissolved in octane. O₂ introduced into the chamber is necessary to reduce the carbon contamination. XPS and HRTEM analysis shows that a Zr silicate layer is formed at the interface during deposition. Although the silicate layer reduces the effective dielectric constant of the gate dielectric, it may provide a better and more stable interface with Si.

The thin ZrO₂ films exhibit good C - V and J - V characteristics. After proper annealing treatments, an equivalent oxide thickness of around 2.3 nm has been achieved for a 5.2 nm thick film, with a leakage current two orders of magnitude lower than that of SiO₂ with the same EOT. The P_b centers in the ZrO₂ films were effectively passivated by FGA. The slight remnant frequency dispersion below midgap might be reduced if a proper FGA were performed after, rather than before gate electrode definition. These electrical properties demonstrate that thin ZrO₂ films formed by Zr(O^{*i*}-Pr)₂(thd)₂ and O₂ might be a promising gate dielectric material for deep submicron CMOS devices if the roughness of the layers and the thickness of the interfacial layer can be reduced. In addition, it might be plausible to apply the thin ZrO₂ films in flash memory as the gate dielectric over the floating gate to increase the coupling ratio. However, further investigation of its reliability is indispensable before using this ZrO₂ film process in CMOS technology.

ACKNOWLEDGMENTS

The authors are grateful to E. Estwick and T. Quance for the assistance in the preparation of the samples. The authors also wish to thank J. R. Hauser for use of the NCSU C - V analysis program. This work was supported by the National Science Council of the Republic of China under Contract No. NSC89-2215-E-009-071.

- ¹The International Technology Roadmap for Semiconductors (Semiconductor Industry Association, 2000).
- ²S.-H. Lo, D. A. Buchanan, Y. Taur, and W. Wang, *IEEE Electron Device Lett.* **18**, 209 (1997).
- ³B. Brar, G. D. Wilk, and A. C. Seabaugh, *Appl. Phys. Lett.* **69**, 2728 (1996).
- ⁴D. J. Hubbard and D. G. Schlom, *J. Mater. Res.* **11**, 2757 (1996).
- ⁵G. D. Wilk, R. M. Wallace, and J. M. Anthony, *J. Appl. Phys.* **89**, 5243 (2001).
- ⁶J. Robertson, *J. Vac. Sci. Technol. B* **18**, 1785 (2000).
- ⁷W.-J. Qi *et al.*, *Tech. Dig. - Int. Electron Devices Meet.*, 145 (1999).
- ⁸W.-J. Qi *et al.*, *Tech. Dig. VLSI Symp.*, 40 (2000).
- ⁹C.-H. Lee *et al.*, *Tech. Dig. - Int. Electron Devices Meet.*, 27 (2000).
- ¹⁰A. C. Jones *et al.*, *Chem. Vap. Deposition* **4**, 46 (1998).
- ¹¹J. R. Hauser and K. Ahmed, *Characterization and Metrology for ULSI Technology: 1998 International Conference*, edited by D. G. Seiler, A. C. Diebold, W. M. Bullis, T. J. Shaffner, R. McDonald, and E. I. Walters (The American Institute of Physics, Melville, N.Y., 1998).
- ¹²S. Iwata and A. Akitoshi, *J. Appl. Phys.* **79**, 6658 (1996).
- ¹³P. Lundgren and M. O. Andersson, *J. Appl. Phys.* **74**, 4780 (1993).
- ¹⁴E. H. Nicollian and J. R. Brews, *MOS (Metal Oxide Semiconductor) Physics and Technology* (Wiley, New York, 1982), p. 465.
- ¹⁵S. M. Sze, *Physics of Semiconductor Devices*, 2nd ed. (Wiley, New York, 1981), p. 403.
- ¹⁶M. Houssa, M. Tuominen, M. Naili, V. Afanas'ev, A. Stesmans, S. Haukka, and M. M. Heyns, *J. Appl. Phys.* **87**, 8615 (2000).